Microplastic exposure induces muscle growth but reduces meat quality and muscle physiological function in chickens

Jiahui Chen, Genghua Chen, Haoqi Peng, Lin Qi, Danlu Zhang, Qinghua Nie, Xiquan Zhang, Wen Luo

PII: S0048-9697(23)01924-1

DOI: https://doi.org/10.1016/j.scitotenv.2023.163305

Reference: STOTEN 163305

To appear in: *Science of the Total Environment*

Received date: 4 February 2023

Revised date: 31 March 2023

Accepted date: 1 April 2023

Please cite this article as: J. Chen, G. Chen, H. Peng, et al., Microplastic exposure induces muscle growth but reduces meat quality and muscle physiological function in chickens, *Science of the Total Environment* (2023), https://doi.org/10.1016/j.scitotenv.2023.163305

Microplastic exposure induces muscle growth but reduces meat quality and muscle physiological function in chickens

Jiahui Chen[2, 3, #], Genghua Chen[2, 3, #], Haoqi Peng[2, 3], Lin Qi[2, 3], Danlu Zhang[2, 3], Qinghua Nie[1, 2, 3], Xiquan Zhang[1, 2, 3], Wen Luo[1, 2, 3, *]

[1] Lingnan Guangdong Laboratory of Agriculture, South China Agricultural University, Guangzhou 510642, China;

[2] Department of Animal Genetics, Breeding and Reproduction, College of Animal Science, South China Agricultural University, Guangzhou 510642, China;

[3] Guangdong Provincial Key Lab of Agro-Animal Genomics and Molecular Breeding, and Key Lab of Chicken Genetics, Breeding and Reproduction, Ministry of Agriculture and Rural Affair, South China Agricultural University, Guangzhou 510642, China;

[#] These authors contributed equally to this work.

[*] **Correspondence:** Wen Luo, College of Animal Science, South China Agricultural University, Guangzhou 510642, Guangdong Province, China

E-mail: luowen729@scau.edu.cn

Abstract

Microplastic (MP) pollution has become one of the global environmental concerns, but the contamination and effect of MP on chicken skeletal muscle are scarcely researched. Here, we found MP contamination in the chicken skeletal muscles, which were directly collected from a large-scale chicken farm. Using Pyrolysis-Gas Chromatography-Mass Spectrometry and Agilent 8700 laser direct infrared imaging spectrometer, we found that polystyrene (PS) and polyamide are the significant type of MPs detected in chicken skeletal muscle. Constant

PS-MP oral feeding for more than 21 days increases the content of MP deposited in chicken breast muscle, but the MP content in the leg muscle was gradually decreased. Surprisingly, the chicken's body and skeletal muscle weight was increased after constant PS-MP feeding. Physiological results showed that PS-MP exposure inhibited energy and lipid metabolism, induced oxidative stress, and potential for neurotoxicity in the skeletal muscle. Metabolomic analysis of the liquid chromatography-tandem mass spectrometry and gas chromatography coupled with the mass spectrometer results showed that PS-MP exposure changed the metabolomic profile and reduced meat quality. In vitro experimental results showed that PS-MP exposure induced chicken primary myoblasts proliferation and apoptosis but decreased myoblasts differentiation. Transcriptome analysis of the skeletal muscle indicates that PS-MP exposure affects skeletal muscle function by regulating genes involved in neural function and muscle development. Considering that chicken is one of the most important meat foods in the world, this study will provide an essential reference for protecting meat food safety.

Keywords: Microplastic pollution; polystyrene microplastics; chicken; muscle growth; meat quality; gene expression.

1. Introduction

Microplastics (MPs) are a type of plastic particle less than 5 mm in diameter deriving from the biodegradable plastics present in the environment (Ragusa et al., 2021). MPs can be accumulated by humans and animals along the food chain, resulting in a significant environmental health issue (Deng et al., 2017). The three major exposure pathways are ingestion, inhalation, and dermal contact (Wu et al., 2022). An adult human may accumulate

approximately 0.9×10^4 to 7.9×10^4 MP items per year (Wu et al., 2022). Evidence has confirmed that MPs exposure poses dangers to human health (Vethaak et al., 2021; Sangkham et al., 2022). Metabolic disturbances, neurotoxicity, and increased cancer risk are all potential consequences of MPs exposure in humans (Vethaak et al., 2021; Sangkham et al., 2022). Studies using mice as a mammalian animal model also showed that exposure to MPs can cause various health problems, such as lipid metabolism disorders and liver inflammation (Lu et al., 2018; Jin et al., 2019). Besides, it is believed that the harmful effects of MPs on humans and animals rely on their size, dose, shape, and chemical composition (Wright et al., 2017; Sangkham et al., 2022). MPs with chemical makeup could cause serious physical and chemical harm to humans and organisms (Wright et al., 2017; Sangkham et al., 2022). The major route of MPs exposure is caused by eating contaminated food, drinks, and drugs. Among them, the intake of microplastics from food is the most. Some previous studies on MPs intake from food mainly concentrate on seafood and aquatic products (Smith et al., 2018; Xu et al., 2020), but few have focused on meat from livestock and poultry, the most consumed protein product in the world.

MPs exposure affects gene expression, cell viability, and tissue development. It has been found that micro- and nano-plastic co-exposure can injure the fetal thalamus by inducing reactive oxygen species (ROS)-mediated cell apoptosis (Yang et al., 2022). However, MPs exposure to human mesenchymal stem cells promoted cell proliferation (Yang et al., 2022), suggesting a controversial role of MPs on cell viability. Besides, short-term MPs exposure also promoted the proliferation of human forebrain cortical spheroids, while long-term exposure inhibited cell viability (Hua et al., 2022). Therefore, MPs negatively affect cell

viability but have a positive role in cell proliferation. In addition to affecting cell growth, MPs can induce tissue damage and inhibit tissue development. The accumulation of MPs in the placenta and fetus of mice induced abnormal morphologies of tissues and reduced fetal weights (Chen et al., 2022). Transcriptome analysis identified that the expression of genes involved in muscle development, lipid metabolism, and skin formation was significantly changed in the placenta and fetal skeletal muscle (Chen et al., 2022). Skeletal muscle accounts for approximately 40% of total body weight (Chen et al., 2022). The skeletal muscle of livestock and poultry is an important source of meat. However, the role of MPs in skeletal muscle growth is currently unclear, and whether exposure to MPs affects livestock and poultry meat production remains to be studied.

Poultry is now the most consumed meat type worldwide (Whitton et al., 2021). Therefore, the safety of poultry meat is important to human health. A previous study has found that MP can accumulate in poultry manure (Wu et al., 2021), and MP contamination was found in chicken meat bought on the market through a polythene-based plastic cutting board the food was cut on (Habib et al., 2022). Nevertheless, the type of MP deposits in the poultry skeletal muscle and their effects on muscle growth has never been studied. Here, we identified the type and concentration of MPs in chicken skeletal muscle using pyrolysis-gas chromatography-mass spectrometry (Py-GC-MS) and laser direct infrared (LDIR) imaging spectrometer. After long-term PS-MP feeding, we found that PS-MP could affect muscle and liver physiological function, meat quality, and muscle growth of chicken. *In vitro* cell experiment results showed that the developmental processes of chicken primary myoblast would be changed after PS-MP exposure. Using transcriptome analysis, we found that PS-MP

affects muscle function by regulating gene expression and alternative splicing related to neural function and muscle development. Our results provide a structural framework for understanding MP's accumulation, regulation, and function in chicken skeletal muscle and provide critical data for elucidating the mechanisms underlying MPs on muscle development and growth.

2. Materials and methods

2.1. Materials

Polystyrene microplastics (PS-MPs) (1.0 % w/v, 10 mL) were purchased from Tianjin Baseline Chromtech Research Centre (Tianjin, China). Three different sizes of PS-MPs (0.5 μm, 5 μm, and 50 μm) were used in this study. The fluorescent PS-MPs (FPS-MPs) were europium chelated, red, and spherical (Fig. S1), and were detectable by spectrofluorimetry (excitation/emission wavelength: 620 nm and 680 nm). The fluorescent dye binds to the surface of the PS-MP and fills inside the microsphere, enabling the fluorescent dye to bind to PS-MP more stable. The solution of FPS-MPs contained 1% suspension in deionized water. The non-fluorescent PS-MPs were white and spherical (Fig. S2). The non-fluorescent stock solution contained 10.17 % suspension in deionized water. The solution of PS-MPs with a diameter of less than 1 μm was added with 0.1 % sodium dodecyl sulfate (SDS) to prevent the MPs from clumping together. PS-MPs suspension was centrifuged at 5000 rpm for 5 min and then washed three times with deionized water to remove the SDS before the exposure experiment. Before exposure, suspended solutions were freshly prepared and sonicated for 30 min in a non-contact ultrasonic water bath (Bioruptor UCD-300 PLUS, Diagenode, Seraing, Belgium).

2.2.Animals and treatment

All the chickens used in this study were directly purchased from a large commercial chicken farm in Guangdong Province. The breed of chicken is Xinghua chicken. For the chickens used in MP detection, three 120-day-old healthy chickens with similar body weights (about 1400 g) were slaughtered and sampled. The tools and storage containers used in the sampling process are all non-plastic.

For the chickens used for PS-MPs feeding, 96 30-day-old chickens with similar body weights (between 250 – 300 g) were randomly assigned to 4 groups (n=24 for each group). One group was used as a negative control and was fed with purified water without PS-MPs. The other three groups were fed with three different sizes (0.5 μm, 5 μm, and 50 μm) of fluorescence PS-MPs solution with 200 μL (0.5mg/mL). To ensure that each chicken takes the same amounts of PS-MPs daily, the PS-MPs were intake by oral gavage. 200 μL PS-MP solution was absorbed by a pipette gun and fed directly into the oral cavity of chickens. Four chickens in each group were randomly selected at 1, 7, 14, 21, 28, and 35 days after feeding and slaughtered for determination. Tissue samples (breast muscle, leg muscle (gastrocnemius muscle), liver, and intestine (ileum) were collected and stored at -80℃.

To evaluate the effect of non-fluorescence PS-MP accumulation in chicken, 15 30-day-old chickens with similar body weight (between 250 – 300 g) were randomly assigned to three groups (n=5 for each group), one group served as the negative control, and the other two groups were fed with 5 μm PS-MPs (0.1mg/day and 0.5mg/day, respectively). The PS-MPs were also intake by oral gavage. The animals were sacrificed after 28 days of continuous feeding for slaughter determination.

The exposure doses of PS-MPs were selected based on previous toxicological studies of PS-MPs in mice and aquatic organisms (Deng et al., 2017; Hou et al., 2021; Lu et al., 2018; Mu et al., 2022). In these previous studies, 0.01 mg/day, 0.1 mg/day, 0.5 mg/day, and 1 mg/day were used to feed the mice. However, a previous study showed that 5 mg/kg (equivalent to feeding 30-day-old chickens with 1.25 mg/day of MPs) MPs would result in high accumulation in mice's tissues and induces severe inflammatory and oxidative stress responses (Choi et al., 2021). Therefore, we chose moderate doses of 0.1 mg/day and 0.5 mg/day for this study.

2.3. Weighing, typing, and counting of MPs by PYGCMS and LDIR

Chicken breast muscle, leg muscle (gastrocnemius muscle), liver, and intestine (ileum) were used to detect the contamination of MP by using pyrolysis gas chromatography/mass spectrometry (PyGCMS). The samples were ground to powder and loaded on a PY-3030D (Frontier Lad, Japan) fast-heating Pt-filament device coupled to a GCMS-QP2020 (SHIMADZU, Japan). The cracking temperature is set at 550℃. A 30-meter RESTEK Rtx-5MS column was used for GC with the temperature program as follows: the initial temperature was at 40℃ and kept for 2 min, then heated up to 320℃ at a rate of 20℃ per minute. This temperature is then kept for 14 min. Ionization of GC is electron impact (EI^+, 70eV, source temperature 230℃). The scanned range of m/z is 40-600. Before sample determination, we added an appropriate amount of nitric acid for digestion for two hours, then added a certain amount of deionized water to ensure that the solution was weakly acidic, and finally dropped it into the PyGCMS sample introduction crucible and test on the machine after the solvent is completely volatilized. Besides, standards of different types of MPs were

tested by PyGCMS to build a quantitative curve (Fig. S3), and the MPs content is calculated according to measure the peak area (Fig. S4; Akoueson et al., 2021). PyGCMS detection was carried out in Shanghai WEIPU Testing Technology Group Co., Ltd. Based on the company's experience, the minimum detectable amount of PS, PET, PMMA, PC, PA6, PA66, and PVC is 0.02 μg, the minimum detectable amount of PP and PE is 0.5 μg, and the minimum detectable amount of PLA and PBAT is 0.2 μg.

Agilent Technologies 8700 laser direct infrared (LDIR) instrument (Chemical Imaging System, Germany) was used to directly analyze and image the shape, size, and chemical composition of microplastic particles in chicken breast muscle samples. The Clarity software version 1.3.9 (Agilent) was used to analyze the results. An infrared scan at 1799 cm^{-1} of the selected sample area on the kevley glass slide (75 × 25 mm, Kevley Technologies, Ohio, US) was performed to locate particles. A high-magnification visible-light camera was used to measure the dimensions of the particles. The instrument then collects a mid-infrared range (1800 cm^{-1} to 975 cm^{-1}) spectrum for each identified particle and then conducts a library search (a microplastic library previously constructed by the Shanghai WEIPU Testing Technology Group Co., Ltd) and provides a match for each particle. The particle identification diameter range was extended to 20-500 μm. The mapping ratio for identification polymers in LDIR is >0.65.

2.4. Histological analysis

The indicated tissues used in this study were placed on a tissue holder and embedded in an optimal cutting temperature compound. Then the samples were frozen rapidly to -20°C, secured on a chuck, and 10 μm sections were cut using CM1950 freezing microtome (Leica,

Germany) with Low-Profile Disposable Blades 819 (Leica, Germany). The cryosections were then fixed on glass slides, added the sealing agent with DAPI was placed at room temperature for 15 s. Finally, the sections were captured with a confocal microscope TCS SP8 (Leica, Germany) within 30 min.

2.5. Quantifying the accumulated concentration of FPS-MPs in chicken skeletal muscle

The frozen samples are thawed at room temperature, and the softened muscle tissues are put into the meat grinder (Supor, China) to be crushed into the meat foam and weighed. Then the samples are flattened and baked in a 60℃ oven overnight. The dried samples were ground into a powder with a high-speed pulverizer (Taisite, China), weighted, and filtered with a 40-mesh metal sieve. About 0.1 g of dry powder was placed in a 4 mL grinding tube. Add 2 mL of normal saline and grind it in a cryogenic grinder (Jingxin, China). The ground program is set as 70hz/120s for 3 times. After centrifugation to remove air bubbles, the solution was transferred to a 6-well plate. A Varioskan LUX multifunctional microplate reader (Thermo, USA) was used to determine the concentrations of MPs in these samples with excitation= 620 nm and emission = 680 nm. Serial dilutions of fluorescent PS-MP suspensions generated the standard curve (Fig. S5). Base on the standard curve, the minimum amount of fluorescent PS-MP that can be detected is 0.5 μg (Fig. S6). To determine the amount of FPS-MP present, the fluorescence intensity was measured and used to calculate its content.

2.6. Physiological analyses of skeletal muscle and liver

Alterations of biomarkers in chicken skeletal muscles and livers due to PS-MPs exposure were determined to evaluate the toxic effects of PS-MPs. The following markers

were included: ATP level and lactate dehydrogenase (LDH) activity for energy metabolism; the total cholesterol (T-CHO) and triglycerides (TG) level for lipid metabolism; the activities of glutathione peroxidase (GSH-Px) and superoxide dismutase (SOD) for oxidative stress; acetylcholinesterase (AChE) activity for neurotoxic responses. All the above markers were detected using commercial kits (Nanjing Jiancheng Bioengineering, Nanjing, China) according to the protocols provided by the manufacturer.

2.7. Metabolomic analysis for LC-MS/MS

50-100 mg of each muscle sample were used for metabolite extraction. 200 μL of precooled water was added to the sample and vortex for 60 s. Next, 800 μL of precooled methanol acetonitrile solution (1: 1, v/v) was added, vortex for another 60 s, and then sonicated for 30 min at low temperature. To precipitate proteins, samples were then incubated at -20°C for 1 h. The suspension was centrifuged at 12000 g at 4°C for 10 min. After centrifugation, the supernatant is transferred to vacuum drying, and the dried precipitates are dissolved in 200 μL of 50% acetonitrile. The solution was then vortexed and centrifuged at 14000 g for 15 min at 4°C. Finally, the supernatant was transferred to 96-well plates for further analysis. The quality control samples were prepared by mixing 10 μL supernatants from each sample.

A Vanquish UPLC system (Thermo, USA) and a Q Exactive HFX mass spectrometer (Thermo, USA) were used for LC-MS/MS analysis. The setting parameters of the UPLC experiment were shown as follows: chromatographic column is Waters HSS T3 (100*2.1 mm, 1.8 μm), mobile phase A is 0.1% formic water solution, mobile phase B is 0.1% formic-acetonitrile. The column temperature was set as 40°C, and a 2 μL sample was used for

the injection. The elution gradient: 0.0-1.0 min A/B (100:0 v/v), 1.0-9.0 min A/B (5:95 v/v), 9-13 min A/B (5:95 v/v), 13.1-17.0 min A/B (100:0 v/v). Electrospray ionization conditions were set as follows: 40 arb for sheath gas flow rate, 10 arb for aux gas flow rate, and spray voltages of the positive and negative modes were 3000 V and 2800 V, respectively. The vaporizer temperature was 350°C, and the capillary temperature was 320°C. The scanning mode was Full-ms-ddMS2. The primary scan m/z range was 70-1050 Da, and the secondary scan m/z range was 200-2000 Da. The primary resolution was 70000, and the second resolution was 17500.

The raw data from LC-MS/MS were analyzed using Progenesis QI (Waters Corporation, Milford, USA) for peak detection, extraction, alignment, and integration. An in-house database and two public databases (http://www.hmdb.ca/ and https://metlin.scripps.edu/) were applied to metabolites annotation. The data processing principles are as follows: (1) Only keep variables with more than 80% non-zero values in any set of samples. (2) Total peak normalization followed by deletion of variables with relative standard deviation (RSD) $\geqslant$ 30% of QC samples. (3) Perform log10 conversion on the data to obtain the final data matrix for subsequent analysis.

The differential metabolites between the two groups were identified using Student's *t*-test with SPSS (27.0). SIMCA software (Sartorius Stedim Data Analytics AB, Umea, Sweden) was used for principal component analysis (PCA) and orthogonal projections to structures-discriminant analysis (OPLS-DA). Value of variable importance in the projection (VIP) $\geq$ 1 and p-value < 0.05 were considered significantly differential metabolites. The heatmaps were constructed using Expression Heat Mapper

(http://www.heatmapper.ca/expression/) with a default parameter.

2.8.Metabolomic analysis for GC-MS

50-100 mg of each muscle sample were used for metabolite extraction. 200 μL of precooled water was added to the muscle sample and then vortex for 60 s. Next, 800 μL of precooled methanol acetonitrile solution (1:1, v/v) was added and vortexed for another 60 s. Then the samples were sonicated for 30 min at 4℃. To precipitate proteins, the samples were incubated at −20℃ for 1 h. The suspension was then centrifuged at 12000 g for 10 min at 4°C, and the supernatant was vacuum dried and dissolved in 200 μL of methoxyamine hydrochloride. Six hours after a 50℃ reaction, 100 μL of MSTFA was added and then reacted at 50°C for 3 h. The solution was then centrifuged at 12000 g for 10 min at 4°C. Finally, transferred the supernatant to 96-well plates for further analysis.

A 7820A-5977B GC-MS instrument (Agilent, DE, USA) was used for GC-MS analysis with HP-5 MS UI column (30 m * 0.25 mm * 0.25 μm). The injection volume was 1 μL. The initial temperature of the column oven was 70 ℃. This temperature was kept for 3 min and then raised to 300 ℃ at a rate of 5 ℃/min. The final temperature was kept for 5 min. Quality control samples were inserted into the sample queue to monitor and evaluate the system stability and the experimental data reliability. Electron ionization (EI) mode was used for MS analysis. The analytes were detected in full SCAN mode. The optimized MS conditions are as follows: transmission line temperature was 290℃, and ion source temperature was 280℃.

Mass Hunter (Agilent) was used for processing the raw data. NIST Online Databases (http://srdata.nist.gov/) was applied to metabolite annotation. The data analysis process is the same as the above LC-MS/MS.

2.9. Cell Culture

As previously described, we isolated primary myoblasts from the chicken leg and breast muscle of the day 10 embryo (Luo et al., 2014). After isolation and purification, myoblasts were then cultured in a growth medium, which consisted of RPMI-1640 (Gibco, Grand Island, NY, USA), 15% FBS (ExCell, Shanghai, China), 10% chicken embryo extract, and 0.2% penicillin/streptomycin (Gibco) at 37℃ in 5% CO_2. To induce differentiation, myoblasts were cultured in a differentiation medium (RPMI-1640 with 2% horse serum) when they reached 90% confluent.

2.10. RNA sequencing (RNA-seq) and data analysis

RNA-seq libraries were performed using ABclonal mRNA-seq Lib Prep Kit (ABlonal, China) according to the manufacturer's instructions. DNBSEQ-T7 system (MGI, China) was then used to sequence the libraries with 150-bp pair-end reads. RNA-seq data from eight chickens have been deposited in the NCBI Sequence Read Archive data repository with accession number PRJNA921954. Quality assessment of reads was analyzed using FASTQC (http://www.bioinformatics.babraham.ac.uk/projects/fastqc/). Trimmomatic software v0.36 was then used to trim the sequences (Bolger et al., 2014). Using STAR software, each data was aligned against the chicken GRCg6a reference genome (Dobin et al., 2013). Read counts of each gene were extracted using STAR –quantMode. Differential gene expression was performed using DESeq2(Love et al., 2014). The differential expressed genes between the two groups were screened with log2 (fold change) > 1 or log2 (fold change) < −1 and with statistical significance (p-value < 0.05). ClusterProfiler was used for Gene functional enrichment (Yu et al., 2012). The Database for Annotation, Visualization and Integrated

Discovery (DAVID, https://david.ncifcrf.gov/tools.jsp/) and R Studio was used for Gene ontology (GO) and Kyoto Encyclopedia of Genes and Genomes (KEGG) analysis of the enriched genes. The alternative splicing events were classified as exon skipping (ES), mutually exclusive exons (MXE), intron retention (IR), alternative 3' splice site (3'ss), and alternative 5' splice site (5'ss). rMATS was used to identify the alternative splicing events (Shen et al., 2014). Differentially spliced events were selected with p-value < 0.05 and abs(lncLeveldiff) > 0.1.

2.11. RNA extraction and quantitative real-time PCR

RNAiso reagent (Takara, Otsu, Japan) was used to extract total RNA from tissues or cells. PrimeScript™ RT reagent Kit (Perfect Real Time) (Takara) was used for the reverse transcription of mRNA according to the manufacturer's manual. Primers specific to each gene were designed and provided in Table S1. qPCR program was carried out in QuantStudio 5 qPCR System (Thermo, CA, USA) with SYBR Green. All reactions were run in triplicate. The relative mRNA expression of genes was calculated using the $2^{-\Delta\Delta Ct}$ method with *β-actin* as a reference.

2.12. Cell proliferation and cell viability analysis

CCK-8: 96-well plates containing the indicated concentration of PS-MP were used for seeding chicken primary myoblasts. Cell proliferation analysis was performed at 12, 24, and 36 h using the Cell counting kit-8 reagent (Dojindo Laboratories, Kumamoto, Japan). iMARK™ Microplate Absorbance Reader (Bio-Rad, California, USA) was used for obtaining the absorbance value at 450 nm.

EdU: Cells seeded in 12-well plates were used in this analysis. After culture with the

indicated concentration of PS-MP for 48 h, 50 μM EdU (RiboBio, China) was added to the cells and incubated for 2 h at 37°C. 4% paraformaldehyde was added and incubated for 30 min to fix the cells. 2 mg/mL glycine solution was used to neutralize cells, and 0.5% Triton X-100 was used to permeabilize cells. Apollo reagents were incubated with cells for 30 min at room temperature. A DAPI solution was used to stain the nuclear. DMi8 fluorescence microscope (Leica, Germany) was used to capture five randomly selected fields for each well.

Cell cycle: Primary myoblasts were cultured in 12-well plates using the growth medium with the indicated concentration of PS-MP. The cells were harvested by trypsin and fixed overnight in 75% ethanol at 4°C after culturing for 48 h. The cell cycle analysis kit (Beyotime, Shanghai, China) was used according to the manufacturer's instructions. BD Accuri C6 flow cytometer (BD Biosciences, USA) was used for flow cytometry analysis, and Modfit LT 5.0 was used for data analysis.

Cell Viability analysis: To measure cell apoptosis, primary myoblasts were seeded into 12-well plates and incubated with membrane permeability (MP)solution with final concentrations of 0.01, 0.1, 1, 5, and 10 μg/mL. After culturing for 48 h, an Annexin V-FITC apoptosis detection kit (Beyotime) was used to stain the cells. BD Accuri C6 flow cytometer was used for cell apoptosis analysis.

2.13. Immunofluorescense

After the density of chicken primary myoblasts reached 90% in a 12-well plate, the growth medium was replaced by a differentiation medium containing 1% bovine serum and indicated a concentration of MP solution. After 48 h differentiation, 0.1% Triton X-100 was

added to the cells for 30 min. Next, goat serum was added and incubated for 1 h at room temperature and then incubated with MyHC antibody (DHSB, USA; 1:100) overnight at 4°C. The FITC-conjugated AffiniPure Goat Anti-Mouse IgG (H + L) (Bioworld, MN, USA; 1:50) was incubated with the cells for 1 h. DAPI was used to stain the nuclear for 15 min. Leica DMi8 fluorescent microscope was used to capture the images.

2.14. Statistical analysis

All results are represented as mean ± sem. For the statistical analysis of the two contrasts, we used an independent sample *t*-test through SPSS. For analysis between multiple groups, we used One-way ANOVA followed by Dunnett's test. $\boldsymbol{p} < 0.05$ was considered to be statistically significant. $*\boldsymbol{p} < 0.05$; $**\boldsymbol{p} < 0.01$.

3. Results

3.1. Microplastic residue can be detected in chicken skeletal muscle

To assess the MPs contamination in broiler farms, we put together a list of all the plastics on the farm that can come into direct or indirect contact with chickens (Fig. 1A). Feed bag outer, chicken coop, and feed tank are made of PP. Water pipes are generally made of PVC. The feed bag inner is made of PA, and the sewing thread of the feed bag is made of nylon (PA6 or PA66). Next, to determine whether MPs could be absorbed and deposited in chicken tissues, we used Pyrolysis-Gas Chromatography-Mass Spectrometry (Py-GC-MS) to detect the number of MPs in the livers, small intestines, leg muscles, and breast muscles from three 120-day-old Xinghua chickens. Results showed that polystyrene (PS) and Polyamide-6 (PA6) were deposited in all of the tested tissues (Table 1). Polyamide-66 (PA66) can be detected in the small intestine and liver, while Polyethylene terephthalate (PET) is only

deposited in the liver in high amounts. PA6 is deposited in a high concentration in the skeletal muscle, with average concentrations of 561.593 mg/kg in the breast muscles and 884.712 mg/kg in the leg muscles (Table 1). As the types of MPs that Py-GC-MS can detect are limited, we used Agilent 8700 laser direct infrared (LDIR) imaging spectrometer to identify more MPs deposited in the muscle. We found 33 types of MPs deposited in chicken breast muscle (Fig. 1B and Table S2). Among them, polyamide is the most abundant MP detected in the muscle (Fig. 1C). Additionally, the smaller the diameter of the MPs, the more they are deposited in the muscle (Fig. 1D). Taken together, these results demonstrated that MPs could be found in large amounts in chicken tissues, especially in skeletal muscles, which humans commonly consume.

3.2. Characterization of microplastic ingestion and accumulation in chicken skeletal muscle

To further understand the deposition pattern of MPs in chicken skeletal muscle, we fed chickens with fluorescence polystyrene MP (FPS-MP) of different sizes. We collected muscle samples at different time points for analysis. The results of fluorescence spectroscopy testing indicated that as time progressed (Fig. 2A), the concentration of FPS-MPs deposited in the leg muscle decreased progressively, indicating a metabolic pathway for MP in chicken skeletal muscle. However, the concentration of FPS-MPs is relatively stable in the breast muscle and tends to rise for 5 μm FPS-MPs (Fig. 2B). For all of the particle sizes tested, the maximal concentrations of 5 μm FPS-MPs accumulated in the skeletal muscle were significantly higher than those of the other size of FPS-MPs (Fig. 2A-2B), indicating that 5 μm FPS-MPs are more likely to be deposited in skeletal muscle. Additionally, frozen section

results further confirmed that 5 μm FPS-MPs could be deposited in the leg and breast muscles (Fig. 2C). The 0.5 μm and 50 μm FPS-MPs were difficult to find in the section (data not shown).

3.3. Microplastic accumulation promotes chicken muscle growth

To identify the effects of MPs accumulation on chicken growth, we fed chickens with FPS-MPs of different sizes and recorded growth traits at different time points for analysis. To our surprise, after 35 consecutive days of feeding FPS-MPs (0.1 mg/d), the body weight, carcass weight, breast muscle weight, leg muscle weight, and the breast muscle rate of chickens all significantly increased in 5 μm FPS-MPs feeding groups than the control group (Fig. 3A-3E). The deposition of other sizes of FPS-MPs can also significantly promote the growth traits of chickens. For example, 0.5 μm FPS-MP can significantly promote breast muscle weight and breast muscle rate (Fig. 3C and 3E), and 50 μm FPS-MP can significantly promote leg muscle weight (Fig. 3D). But these effects were only observed after 35 days, indicating that the effect of FPS-MP on muscle growth is slow. On the other hand, although there was no significant change in carcass percentage and leg muscle rate between groups, their values tended to increase after 35 consecutive days FPS-MPs feeding compared to the control group (Fig. 3F-3G).

Besides, we also used 5 μm non-fluorescent PS-MPs (0.1 mg/d and 0.5 mg/d) to feed chickens for 28 consecutive days. Results showed that 0.5 mg/d non-fluorescent 5 μm PS-MP feeding significantly increased breast and leg muscle weights. However, the live and carcass weights have no significant difference (Fig. 3H-3K). The higher the concentration of non-fluorescent PS-MPs feeding, the greater the promotion effect on chicken muscle growth

traits (Fig. 3J-3K). However, there were no significant changes in carcass percentage, breast muscle rate, and leg muscle rate between groups (Fig. 3L-3N), suggesting that PS-MPs had a tissue-specific effect on chicken tissue growth. Taken together, PS-MP accumulation in chickens can increase muscle growth.

3.4. Effects of microplastic accumulation on skeletal muscle and liver physiological function

To explore the effects of PS-MP accumulation on the physiological function of chicken skeletal muscle, we fed chickens with two different amounts (0.1 mg/day and 0.5 mg/day) of 5 μm PS-MPs for 28 consecutive days. Results showed that PS-MPs feeding inhibited skeletal muscle energy metabolism. PS-MPs induced a significant decrease in ATP level in a dose-dependent manner. A slight decrease in the lactate dehydrogenase (LDH) activity (Fig. 4A). For lipid metabolism, a significant decrease in the levels of total cholesterol (T-CHO) and triglycerides (TG) were observed after PS-MPs feeding (Fig. 4B), indicating that PS-MPs feeding affect lipid metabolism. For biomarkers of oxidative stress: PS-MPs feeding did not affect superoxide dismutase (SOD) activity, but the activity of glutathione peroxidase (GSH-Px) was increased (Fig. 4C). In addition, the potential for neurotoxicity was evaluated based on the activity of acetylcholinesterase (AChE), which decreased after exposure to 0.5 mg/d PS-MPs (Fig. 4D).

The liver is an important metabolic organ and plays a critical role in the growth and development of animals. Several recent studies have shown frequent loss of muscle mass in liver dysfunction and chronic liver diseases (De Bandt et al., 2018). Our above results showed that 5 μm PS-MPs could accumulate the largest amount in livers. We also did

biological analyses of the liver to test the effects of PS-MP accumulation on liver physiological function. Results showed that PS-MPs feeding has no significant effect on liver energy metabolism (Fig. 4E) but can increase the amount of lipid metabolism markers (Fig. 4F). For biomarkers of oxidative stress: PS-MP feeding did not affect the activity of liver SOD. However, the activity of GSH-Px was reduced (Fig. 4G). Finally, the potential for neurotoxicity was evaluated based on the activity of AChE, which increased after exposure to 0.5 mg/d PS-MPs (Fig. 4H). The above results indicate that PS-MP accumulation significantly affects chickens' skeletal muscle and liver physiological function.

3.5. Microplastic feeding reduces chicken meat quality

We tested the meat quality after PS-MPs feeding for 35 d. We found that PS-MPs feeding significantly reduced breast muscle shear force and increased leg muscle PH value. The drip loss also declines (Fig. 5A). Muscle metabolites are important regulators of muscle function, growth, and meat quality. To explore the effects of MPs on muscle metabolome, we used liquid chromatography-tandem mass spectrometry (LC-MS/MS) and gas chromatography coupled to the mass spectrometer (GC-MS) to analyze chicken skeletal muscle metabolism and meat flavors, respectively, after 5 μm PS-MPs feeding for 35 consecutive days. 381 metabolites were quantified from breast muscle samples using LC-MS/MS (Table S3). These metabolites can be grouped into 22 categories (Fig. 5B). PCA (Fig. 5C) and PLS-DA (Fig. 5D) showed that there are differences in the muscle metabolite profiles between PS-MPs feeding and control groups. We performed pairwise comparisons between groups to identify significantly altered metabolites by PS-MPs. To our surprise, only two metabolites were altered considerably (Fig. 5E), including D-Tagatose 1-phosphate and

nicotinamide (Fig. 5F). Both tagatose and nicotinamide have positive effects on improving meat quality (Bautista et al., 2000; Wu et al., 2020). Additionally, the relative abundance of inosinic acid (IMP), a famous flavor substance for meat quality (Zhang et al., 2008), was also reduced after PS-MPs were exposed (Fig. 5G). Inosine and hypoxanthine (Liu et al., 2021), two IMP by-products negatively affecting meat quality, exhibited an increasing trend after PS-MPs exposure (Fig. 5G). Therefore, PS-MPs feeding may affect chicken meat quality.

To further determine whether PS-MP feeding affected meat quality, meat flavor compounds were detected. 237 flavor metabolites were quantified from breast muscle samples using GC-MS (Table S3). These metabolites can be grouped into 20 categories (Fig. 5H). PCA (Fig. 5I) and PLS-DA (Fig. 5J) showed differences in the meat flavor metabolite profiles between PS-MPs feeding and control groups. Pairwise comparison results showed seven metabolites significantly altered after PS-MP feeding (Fig. 5K-5L). Notably, all these seven metabolites were decreased considerably after exposed to PS-MPs, and some of them are important flavor substances and are involved in the formation of chicken flavor, such as decanal, 13-Docosenamide, and carbonic acid (Lorenzo et al., 2021; Pavlidis et al., 2021; Terzi et al., 2021). The above results indicate that PS-MPs feeding had little effect on the metabolomic profile of skeletal muscle. However, some metabolites and flavor compounds related to chicken meat quality can be inhibited after PS-MP exposure.

3.6. Microplastics induced myoblasts proliferation and apoptosis but decreased myoblasts differentiation

To further understand how MPs affect muscle development, we added PS-MPs to chicken primary myoblasts (CPMs) and examined their effect on cell activity. We found that

5 μm PS-MPs can be absorbed by the CPMs (Fig. 6A). The expression of muscle differentiation marker genes can be inhibited by different concentrations of PS-MPs (Fig. 6B-6D), and the differentiation index and myotube formation were also be repressed by adding of PS-MPs (Fig. 6E-6G). Surprisingly, adding PS-MPs promoted gene expression in cell proliferation and increased cell viability (Fig. 6H-6K). 5-ethynyl-2'-deoxyuridine (EdU) staining also showed that PS-MPs addition increased the percentage of proliferation cells (Fig. 6L-6M). Therefore, PS-MPs can increase CPMs proliferation but decrease CPMs differentiation. On the other hand, PS-MPs addition significantly inhibited the expression of *BCL-2* and *BAK* (Fig. 6N-6O), two important cell apoptosis marker genes. Flow cytometry assay further confirmed that PS-MPs exposure promoted cell apoptosis (Fig. 6P-6Q). The above results indicated that PS-MPs induced CPMs proliferation and apoptosis but decreased CPMs differentiation.

3.7. Transcriptome analysis reveals that PS-MP exposure affects chicken skeletal muscle function by regulating genes involved in neural function and muscle cell development

To explore the potential mechanism underlying PS-MP regulation on chicken skeletal muscle growth, we collected skeletal muscle from chickens fed 5 μm PS-MPs for 35 consecutive days and used RNA sequencing (RNA-seq) to analyze gene expression. 121 genes were significantly differentially expressed between PS-MPs exposed muscles and control muscles (Fig. 7A and Table S4). Among these differentially expressed genes (DEGs), 54 genes were up-regulated, and 67 genes were down-regulated (Fig. 7B). KEGG analysis showed that neuroactive ligand-receptor interaction and circadian rhythm are two

significantly enriched pathways (Fig. 7C). These two pathways are all directly related to neural function (Patke et al., 2020; Wei et al., 2020). GO analysis also showed that many GO terms related to neural function were significantly enriched, such as circadian rhythm, chemical synaptic transmission, and synaptic cleft (Fig. 7D). GO terms involved in muscle development are also enriched in this analysis, such as skeletal muscle cell differentiation and negative regulation of cell adhesion (Fig. 7D).

Alternative splicing is essential for regulating gene expression and increasing proteome diversity (Chen et al., 2009). Here, we also analyze the change of mRNA alternative splicing between PS-MPs exposed muscles and the control muscles. We found that 564 genes were significantly differentially splicing between the two groups (Table S4). Skipped exon (SE), which accounts for 77.41%, is the main differentially splicing type (Fig. 7E). KEGG and GO analysis found that the differentially splicing genes (DSGs) were also enriched in pathways and GO terms involved in neural function, such as axon guidance, modulation of synaptic transmission, synapse maturation, neurogenesis, and neuronal cell body (Fig. 7F-7G, Table S5). Only two genes were both significantly differentially expressed and differentially splicing between the two groups (Fig. 7H). Then, we performed GO and KEGG analysis for DEG and DSG together. Similar to the above results, many pathways and GO terms involved in neural function were enriched in the analysis results, such as axon guidance, circadian rhythm, nervous system development, neuron projection development, and modulation of synaptic transmission (Fig. S7 and Table S6). Finally, gene set enrichment analysis (GSEA) of the RNA-seq data further showed that PS-MPs exposure resulted in the positive enrichment of neural function-related GO terms and KEGG pathway (Fig. 7I). Some GO

term and KEGG pathways involved in muscle development were also positively enriched in the GSEA results (Fig. 7J). T above data suggest that PS-MP exposure affects skeletal muscle function by regulating genes involved in neural function and muscle development.

4. Discussion

Plastics are a broad definition of various synthetic or natural high polymers. Various plastics are closely related to human production and life. Still, plastics are difficult to biodegradable and can only be digested into micro or nano-sized particles through physical processes, requiring decades or even centuries to degrade (Krivokonsky et al., 2018). This characteristic has led more and more scholars to start paying attention to the impact of MPs on organisms (Rillig et al., 2020; Yuan et al., 2022). MPs also carry toxic chemicals, including toxic additives and heavy metals (Tiwari et al., 2019). Less than 150 μm plastic particles can be absorbed by organisms into the body, even into cells (Yuan et al., 2022), and accumulated through the biological chain. In the earthworm (*Eisenia andrei*), ingesting microplastics can cause congestion and inflammatory infiltration (Rodriguez-Seijo et al., 2017). In sea bass (*Dicentrarchus labrax*), long-term intake of PVC-MP can lead to moderate to severe histopathological changes in the intestine (Pedà et al., 2016). In the zebrafish model, exposure to environmental-related concentrations (1-100 μg/L) of PS-NPs can lead to intestinal immune dysfunction and alter the structure and function of intestinal flora (Teng et al., 2022). PS-NPs can also cause carditis and cardiomyocyte apoptosis in carp (Wu et al., 2022). These studies have shown that a certain amount of MPs intake harms animal bodies.

Increasing evidence has suggested MP pollution in livestock and poultry farm. A previous study identified MPs contamination in manure and feed (Wu et al., 2021). A recent

study further found that some MPs from supermarket cutting boards can accumulate in chicken meat. Nevertheless, no study has shown MPs in livestock and poultry, especially meat. Our results are the first to confirm the presence of MPs residues in poultry, the most-eaten meat in the world. For the pollution sources of these MPs in poultry, we suspect that they will likely come from feed or the packaging membrane of the feed. The chickens we collected were caged and could not eat plastic waste in the environment. Our results showed that PA6 and PA66 are the MPs that remain the most in chickens. Both of these substances belong to nylon. Of all the sources of plastic pollution we have observed in chicken farms, only the inner membrane of the feed bag is made of nylon. The inner membrane of the feed bag is in direct contact with the feed, and the friction between the plastic bag and the feed during transportation promotes the release of MPs into the feed. The high temperature in South China may also intensify the process of releasing MPs into the feed (Zha et al., 2022). Therefore, feed manufacturers should think of ways to reduce plastic pollution in feed packaging bags.

Metabolome analysis is emerging as a useful tool for assessing meat quality and meat safety (Zhang et al., 2021). Many metabolites are related to meat quality traits. For example, an untargeted metabolomics method based on UHPLC-MS was developed to assess meat freshness in chickens. Some metabolites, such as tyramine, indole-3-carboxaldehyde, and L-anserine, were identified as freshness-related biomarkers (Wen et al., 2020; Zhang et al., 2020). A metabolomics method based on nuclear magnetic resonance or GC-MS can assess meat's freshness and predict the meat's storage time (Argyri et al., 2015; Castejon et al., 2015). Here, we detected the effects of PS-MP exposure on chicken meat quality using LC-MS and

GC-MS. However, only 9 metabolites were significantly changed after PS-MP exposure, suggesting that PS-MP exposure has little effect on meat metabolomics and quality.

On the other hand, the abundance of all 9 metabolites was significantly inhibited after PS-MP exposure. Some metabolites, such as D-tagatose, nicotinamide, and decanal, were related to meat quality. D-tagatose can inhibit the growth of microorganisms in meat products, and the spoilage rate of the meat products can also be decreased by D-tagatose (Bautista et al., 2000). Dietary supplementation with nicotinamide can improve the meat quality of broilers (Wu et al., 2020). Decanal was correlated with meat's freshness (Pavlidis et al., 2021). The inhibition of PS-MPs exposure to these metabolites would reduce meat quality. Besides, as meat is an important food for humans, the MPs in the meat would affect meat safety and human health. Many chemicals sorbed to MPs are known to be potent toxicants in humans, triggering adverse effects such as neurological disorders, endocrine disruption, and reduced reproductive success (Hantoro et al., 2019). Raising people's attention to meat MP residues and assessing their potential harm to humans will be the next step for researchers.

An important finding of this study is that we found PS-MP feeding not only induced myoblast proliferation but also increased chicken body weight. The positive effect of PS-MPs on cell proliferation has been reported in many studies. For human cells, short-term PS-MP exposure promoted pluripotent stem cell proliferation (Hua et al., 2022). A promotion effect of cell proliferation was also shown in human mesenchymal stem cells after PS-MP exposure (Im et al., 2022). For cells of other species, nano plastics can stimulate the proliferation of swine granulosa cells at a high concentration, while cell viability results are unaffected (Im et al., 2022). Polyethene MPs can cause mucous cell proliferation in carp gills (Cao et al., 2022).

However, some other studies showed that MP could inhibit cell proliferation. Exposure to PS-MPs in human embryonic kidney and hepatocellular liver cells significantly reduced cellular proliferation (Goodman et al., 2022). Based on the above contradictory results, we speculate that the effect of MP on cell proliferation may be related to the size, shape, concentration, material, and zeta potential of MP or even the target cell type.

The promoted effect of PS-MPs feeding on chicken growth was surprising to us. Because previous studies have believed that MP is toxic to animals and humans (Waring et al., 2018; Lu et al., 2018), our two feeding experiments, which lasted for about one month, showed that MP feeding did promote body growth in chickens. The *in vitro* cell experiments also supported this result. MP exposure induced myoblast proliferation and apoptosis. The proliferation of myoblast is beneficial for skeletal muscle growth (Waring et al., 2018; Lu et al., 2018), while proper cell apoptosis favors myogenesis (Jiang et al., 2021). Deposition of MPs in muscle may stimulate myoblast proliferation and myogenesis process, thereby promoting muscle growth. However, the detailed mechanism underlying the promoted effect of MPs on chicken growth still needs further exploration. More *in vivo* and *in vitro* experiments are needed to confirm and analyze the role of MPs in chickens.

Our transcriptome results found that the expression and alternative splicing of many genes involved in neural function were significantly changed after PS-MP exposure. Physiology function analysis of skeletal muscle also showed that PS-MP exposure induced neurotoxicity. The neural function is important for maintaining muscle mass and muscle function. Nerve impulses can initiate muscle contraction, and the denervation of muscle fibers can cause muscle atrophy (Cisterna et al., 2014). Neural continuity disruption could

also cause adverse effects on muscle biology (Cisterna et al., 2014). Many genes and pathways, such as the circadian rhythm, were related to neural function. Circadian rhythms are established and maintained by the suprachiasmatic nucleus, composed of approximately 20,000 neurons (Reppert et al., 2001; Masri et al., 2013). Our results found that the circadian rhythm is significantly enriched in the DEGs between PS-MP exposure and control groups, indicating that PS-MP exposure may affect circadian rhythm. A recent study found that the circadian rhythm controls the metabolism of amino acids in murine skeletal muscle. The knock-out of circadian rhythm genes disrupts the hypertrophy of skeletal muscle in mice (Aoyama et al., 2021). Therefore, regulating the circadian rhythm pathway may be one of the reasons that PS-MP affects muscle growth and function in chickens. Axon guidance is another significantly enriched pathway in our RNA-seq result.

The proper formation of neuronal connections during development requires axon guidance (Van Vactor et al., 1999). Notably, some axon guidance molecules are involved in myogenesis. A recent study has shown that repulsive guidance molecule a (RGMa), a GPI-anchor axon guidance molecule, is expressed in skeletal muscle cells. Overexpression of RGMa induces hypertrophy of muscle cells (Copola et al., 2022). Neogenin plays a key role in axon guidance by interacting with RGMs and netrin-1 (Copola et al., 2022). It has been found that neogenin can regulate myogenic differentiation and skeletal myofiber size (Bae et al., 2009). Mice with *neogenin* mutation have abnormally small myofibers at embryonic day (Bae et al., 2009). Therefore, considering that neural toxicity of MP was also found in cultured neural stem cells, fish, mice, and many other marine organisms (Deng et al., 2017; Jeong et al., 2022; Teng et al., 2022), one of the mechanisms by which PS-MP affects

chicken muscle growth and function may be through its neurotoxicity.

5. Conclusions

Microplastic residue can be detected in chickens' small intestines, liver, and skeletal muscles. The smaller the diameter of the MPs, the more they are deposited in the skeletal muscle. PS-MP exposure inhibited the energy metabolism and lipid metabolism of skeletal muscle, induced oxidative stress, and potential for neurotoxicity of skeletal muscle. The metabolomics results show that PS-MPs may affect meat quality by inhibiting the abundance of metabolites related to meat quality. *In vivo* and *in vitro* results show that PS-MP exposure promotes chicken muscle growth and induces myoblast proliferation and apoptosis. Transcriptome results suggest that PS-MP exposure affects skeletal muscle function by regulating genes involved in neural function and muscle development.

This work is the first to report the contamination and function of MPs in poultry skeletal muscle. As poultry is a vital meat source for humans, the roles of MP on chicken growth, quality, and safety should be paid more and more attention in future research.

Credit authorship contribution statement

Wen Luo conceived and supervised the project. Wen Luo, Jiahui Chen, and Genghua Chen designed the research. Jiahui Chen, Genghua Chen, Haoqi Peng, Lin Qi, and Danlu Zhang performed experiments. Xiquan Zhang and Qinghua Nie refined the language of the manuscript and supplemented the experiment. Wen Luo, Jiahui Chen, and Genghua Chen analyzed the data and wrote the manuscript.

Declaration of Competing Interest

The authors declare that they have no known competing financial interests or personal

relationships that could have appeared to influence the work reported in this paper.

Acknowledgments

This work was supported by National Key Research and Development Program of China (2022YFF1000201), Natural Scientific Foundation of China (31972544, 32272861), Guangdong Special Branch Plans of Young Talent with Scientific and Technological Innovation (2019TQ05N470), China Agriculture Research System of MOF and MARA (CARS-41), and the Local Innovative and Research Teams Project of Guangdong Province (2019BT02N630).

Institutional Review Board Statement

This study was conducted according to the guidelines of the Declaration of Helsinki and approved by South China Agricultural University Institutional Animal Care and Use Committee (approval number: SCAU#2022A031).

Conflict of interest

The authors declare no conflict of interest.

References:

Akoueson F., Chbib C., Monchy S., Paul-Pont I., Doyen P., Dehaut A., Duflos G., 2021. Identification and quantification of plastic additives using pyrolysis-GC/MS: A review. The Science of the total environment, 773, 145073.

Aoyama S., Kim H. K., Hirooka R., Tanaka M., Shimoda T., Chijiki H., Kojima S., Sasaki K., Takahashi K., Makino S., Takizawa M., Takahashi M., Tahara Y., Shimba S., Shinohara K., Shibata S., 2021. Distribution of dietary protein intake in daily meals influences skeletal muscle hypertrophy via the muscle clock. Cell Rep 36 (1): 109336.

Argyri A. A., Mallouchos A., Panagou E. Z., Nychas G. J., 2015. The dynamics of the HS/SPME-GC/MS as a tool to assess the spoilage of minced beef stored under different packaging and temperature conditions. Int J Food Microbiol 193: 51-58.

Bae G. U., Yang Y. J., Jiang G., Hong M., Lee H. J., Tessier-Lavigne M., Kang J. S., Krauss R. S., 2009. Neogenin regulates skeletal myofiber size and focal adhesion kinase and extracellular signal-regulated kinase activities in vivo and in vitro. Mol Biol Cell 20 (23): 4920-4931.

Basini G., Bussolati S., Andriani L., Grolli S., Ramoni R., Bertini S., Iemmi T., Menozzi A., Berni P., Grasselli F., 2021. Nanoplastics impair in vitro swine granulosa cell functions. Domest Anim Endocrinol 76: 106611.

Bautista D. A., Pegg R. B., Shand P. J., 2000. Effect of D-glucose and D-tagatose on bacterial growth in media and a cooked cured ham product. J Food Prot 63 (1): 71-77.

Bolger A. M., Lohse M., Usadel B., 2014. Trimmomatic: a flexible trimmer for Illumina sequence data. Bioinformatics 30 (15): 2114-2120.

Cao J., Xu R., Wang F., Geng Y., Xu T., Zhu M., Lv H., Xu S., Guo M. Y., 2022. Polyethylene microplastics trigger cell apoptosis and inflammation via inducing oxidative stress and activation of the NLRP3 inflammasome in carp gills. Fish Shellfish Immunol 132: 108470.

Castejon D., Garcia-Segura J. M., Escudero R., Herrera A., Cambero M. I., 2015. Metabolomics of meat exudate: Its potential to evaluate beef meat conservation and aging. Anal Chim Acta 901: 1-11.

Chen G., Xiong S., Jing Q., van Gestel CAM, van Straalen N. M., Roelofs D., Sun L., Qiu H., 2022. Maternal exposure to polystyrene nanoparticles retarded fetal growth and triggered metabolic disorders of placenta and fetus in mice. Sci Total Environ 854: 158666.

Chen M., Manley J. L., 2009. Mechanisms of alternative splicing regulation: insights from molecular and

genomics approaches. Nat Rev Mol Cell Biol 10 (11): 741-754.

Choi, Y. J., Park, J. W., Lim, Y., Seo, S., & Hwang, D. Y., 2021. In vivo impact assessment of orally administered polystyrene nanoplastics: biodistribution, toxicity, and inflammatory response in mice. Nanotoxicology, 15(9), 1180–1198.

Cisterna B. A., Cardozo C., Saez J. C., 2014. Neuronal involvement in muscular atrophy. Front Cell Neurosci 8: 405.

Copola AGL, Dos Santos IGD, Coutinho L. L., Del-Bem LEV, de Almeida Campos-Junior PH, Da Conceicao IMCA, Nogueira J. M., Do Carmo Costa A., Silva GAB, Jorge E. C., 2022. Transcriptomic characterization of the molecular mechanisms induced by RGMa during skeletal muscle nuclei accretion and hypertrophy. BMC Genomics 23 (1): 188.

De Bandt J. P., Jegatheesan P., Tennoune-El-Hanaa N., 2018. Muscle Loss in Chronic Liver Diseases: The Example of Nonalcoholic Liver Disease. Nutrients 10 (9).

Deng Y., Zhang Y., Lemos B., Ren H., 2017. Tissue accumulation of microplastics in mice and biomarker responses suggest widespread health risks of exposure. Sci Rep 7: 46687.

Dobin A., Davis C. A., Schlesinger F., Drenkow J., Zaleski C., Jha S., Batut P., Chaisson M., Gingeras T. R., 2013. STAR: ultrafast universal RNA-seq aligner. Bioinformatics 29 (1): 15-21.

Goodman K. E., Hua T., Sang Q. A., 2022. Effects of Polystyrene Microplastics on Human Kidney and Liver Cell Morphology, Cellular Proliferation, and Metabolism. ACS Omega 7 (38): 34136-34153.

Habib R. Z., Kindi R. A., Salem F. A., Kittaneh W. F., Poulose V., Iftikhar S. H., Mourad A. I., Thiemann T., 2022. Microplastic Contamination of Chicken Meat and Fish through Plastic Cutting Boards. Int J Environ Res Public Health 19 (20).

Hantoro I., Lohr A. J., Van Belleghem FGAJ, Widianarko B., Ragas AMJ., 2019. Microplastics in coastal areas

and seafood: implications for food safety. Food Addit Contam Part A Chem Anal Control Expo Risk Assess 36 (5): 674-711.

Hua T., Kiran S., Li Y., Sang Q. A., 2022a. Microplastics exposure affects neural development of human pluripotent stem cell-derived cortical spheroids. J Hazard Mater 435: 128884.

Hua T., Kiran S., Li Y., Sang Q. A., 2022b. Microplastics exposure affects neural development of human pluripotent stem cell-derived cortical spheroids. J Hazard Mater 435: 128884.

Im G. B., Kim Y. G., Jo I. S., Yoo T. Y., Kim S. W., Park H. S., Hyeon T., Yi G. R., Bhang S. H., 2022a. Effect of polystyrene nanoplastics and their degraded forms on stem cell fate. J Hazard Mater 430: 128411.

Im G. B., Kim Y. G., Jo I. S., Yoo T. Y., Kim S. W., Park H. S., Hyeon T., Yi G. R., Bhang S. H., 2022b. Effect of polystyrene nanoplastics and their degraded forms on stem cell fate. J Hazard Mater 430: 128411.

Jeong B., Baek J. Y., Koo J., Park S., Ryu Y. K., Kim K. S., Zhang S., Chung C., Dogan R., Choi H. S., Um D., Kim T. K., Lee W. S., Jeong J., Shin W. H., Lee J. R., Kim N. S., Lee D. Y., 2022. Maternal exposure to polystyrene nanoplastics causes brain abnormalities in progeny. J Hazard Mater 426: 127815.

Jiang A., Guo H., Wu W., Liu H., 2021. The Crosstalk between Autophagy and Apoptosis Is Necessary for Myogenic Differentiation. J Agric Food Chem 69 (13): 3942-3951.

Jin Y., Lu L., Tu W., Luo T., Fu Z., 2019. Impacts of polystyrene microplastic on the gut barrier, microbiota and metabolism of mice. Sci Total Environ 649: 308-317.

Lee J. K., Hallock P. T., Burden S. J., 2017. Abelson tyrosine-protein kinase 2 regulates myoblast proliferation and controls muscle fiber length. Elife 6.

Liu T., Mo Q., Wei J., Zhao M., Tang J., Feng F., 2021. Mass spectrometry-based metabolomics to reveal chicken meat improvements by medium-chain monoglycerides supplementation: Taste, fresh meat quality, and composition. Food Chem 365: 130303.

Lorenzo Rodrigo A., Tomac Alejandra, Tapella Federico, Yeannes María I., Romero M. Carolina, 2021. Biochemical and quality parameters of southern king crab meat after transport simulation and re-immersion. Food Control 119: 107480.

Love M. I., Huber W., Anders S., 2014. Moderated estimation of fold change and dispersion for RNA-seq data with DESeq2. Genome Biol 15 (12): 550.

Lu L., Wan Z., Luo T., Fu Z., Jin Y., 2018a. Polystyrene microplastics induce gut microbiota dysbiosis and hepatic lipid metabolism disorder in mice. Sci Total Environ 631-632: 449-458.

Lu L., Wan Z., Luo T., Fu Z., Jin Y., 2018b. Polystyrene microplastics induce gut microbiota dysbiosis and hepatic lipid metabolism disorder in mice. Sci Total Environ 631-632: 449-458.

Luo W., Nie Q., Zhang X., 2013. MicroRNAs involved in skeletal muscle differentiation. J Genet Genomics 40 (3): 107-116.

Luo W., Wu H., Ye Y., Li Z., Hao S., Kong L., Zheng X., Lin S., Nie Q., Zhang X., 2014. The transient expression of miR-203 and its inhibiting effects on skeletal muscle cell proliferation and differentiation. Cell Death Dis 5: e1347.

Masri S., Sassone-Corsi P., 2013. The circadian clock: a framework linking metabolism, epigenetics and neuronal function. Nat Rev Neurosci 14 (1): 69-75.

Patke A., Young M. W., Axelrod S., 2020. Molecular mechanisms and physiological importance of circadian rhythms. Nat Rev Mol Cell Biol 21 (2): 67-84.

Pavlidis D. E., Mallouchos A., Nychas G. J., 2021. Microbiological assessment of aerobically stored horse fillets through predictive microbiology and metabolomic approach. Meat Sci 172: 108323.

Pedà C., L. Caccamo, M. C. Fossi, F. Gai, F. Andaloro, L. Genovese, A. Perdichizzi, T. Romeo, G. Maricchiolo., 2016. Intestinal alterations in European sea bass Dicentrarchus labrax (Linnaeus, 1758) exposed to

microplastics: Preliminary results. Environ Pollut 212:251-256.

Piestun Y., Yahav S., Halevy O., 2015. Thermal manipulation during embryogenesis affects myoblast proliferation and skeletal muscle growth in meat-type chickens. Poult Sci 94 (10): 2528-2536.

Pivokonsky M., Cermakova L., Novotna K., Peer P., Janda V., 2018. Occurrence of microplastics in raw and treated drinking water. Science of The Total Environment, 643.

Ragusa A., Svelato A., Santacroce C., Catalano P., Notarstefano V., Carnevali O., Papa F., Rongioletti MCA, Baiocco F., Draghi S., D'Amore E., Rinaldo D., Matta M., Giorgini E., 2021. Plasticenta: First evidence of microplastics in human placenta. Environ Int 146: 106274.

Rahman A., Sarkar A., Yadav O. P., Achari G., Slobodnik J., 2021. Potential human health risks due to environmental exposure to nano- and microplastics and knowledge gaps: A scoping review. Sci Total Environ 757: 143872.

Reppert S. M., Weaver D. R., 2001. Molecular analysis of mammalian circadian rhythms. Annu Rev Physiol 63: 647-676.

Rillig M. C., Lehmann, A., 2020. Microplastic in terrestrial ecosystems. Science, 368(6498), 1430-1431.

Rodriguez-Seijo A., J. Lourenço, T. A. P. Rocha-Santos, J. Da Costa, A. C. Duar, H. Vala, R. Pereira. 2017. Histopathological and molecular effects of microplastics in Eisenia andrei Bouché. Environ Pollut 220:495-503

Sangkham S., Faikhaw O., Munkong N., Sakunkoo P., Arunlertaree C., Chavali M., Mousazadeh M., Tiwari A., 2022. A review on microplastics and nanoplastics in the environment: Their occurrence, exposure routes, toxic studies, and potential effects on human health. Mar Pollut Bull 181: 113832.

Shen S., Park J. W., Lu Z. X., Lin L., Henry M. D., Wu Y. N., Zhou Q., Xing Y., 2014. rMATS: robust and flexible detection of differential alternative splicing from replicate RNA-Seq data. Proc Natl Acad Sci U S

A 111 (51): E5593-E5601.

Smith M., Love D. C., Rochman C. M., Neff R. A., 2018. Microplastics in Seafood and the Implications for Human Health. Curr Environ Health Rep 5 (3): 375-386.

Teng M., Zhao X., Wang C., Wang C., White J. C., Zhao W., Zhou L., Duan M., Wu F., 2022. Polystyrene Nanoplastics Toxicity to Zebrafish: Dysregulation of the Brain-Intestine-Microbiota Axis. ACS. Nano. 16 (5): 8190-8204.

Teng M., Zhao X., Wang C., Wang C., White J. C., Zhao W., Zhou L., Duan M., Wu F., 2022. Polystyrene Nanoplastics Toxicity to Zebrafish: Dysregulation of the Brain Intestine-Microbiota Axis. ACS Nano 16 (5): 8190-8204.

Terzi E., Kucukkosker B., Bilen S., Kenanoglu O. N., Coruh O., Ozbek M., Parug S. S., 2021. A novel herbal immunostimulant for rainbow trout (Oncorhynchus mykiss) against Yersinia ruckeri. Fish Shellfish Immunol 110: 55-66.

Tiwari M., Rathod T. D., Ajmal P. Y., Bhangare R. C., Sahu S. K., 2019. Distribution and characterization of microplastics in beach sand from three different Indian coastal environments. Marine Pollution Bulletin, 140(MAR.), 262-273.

Van Vactor D. V., Lorenz L. J., 1999. Neural development: The semantics of axon guidance. Curr Biol 9 (6): R201-R204.

Vethaak A. D., Legler J., 2021. Microplastics and human health. Science 371 (6530): 672-674.

Waring R. H., Harris R. M., Mitchell S. C., 2018. Plastic contamination of the food chain: A threat to human health? Maturitas 115: 64-68.

Wei J., Liu J., Liang S., Sun M., Duan J., 2020. Low-Dose Exposure of Silica Nanoparticles Induces Neurotoxicity via Neuroactive Ligand-Receptor Interaction Signaling Pathway in Zebrafish Embryos. Int J

Nanomedicine 15: 4407-4415.

Wen D., Liu Y., Yu Q., 2020. Metabolomic approach to measuring quality of chilled chicken meat during storage. Poult Sci 99 (5): 2543-2554.

Whitton C., Bogueva D., Marinova D., Phillips CJC., 2021. Are We Approaching Peak Meat Consumption? Analysis of Meat Consumption from 2000 to 2019 in 35 Countries and Its Relationship to Gross Domestic Product. Animals (Basel) 11 (12).

Wilson N. H., Key B., 2006. Neogenin interacts with RGMa and netrin-1 to guide axons within the embryonic vertebrate forebrain. Dev Biol 296 (2): 485-498.

Wright S. L., Kelly F. J., 2017. Plastic and Human Health: A Micro Issue? Environ Sci Technol 51 (12): 6634-6647.

Wu H., J. Guo, Y. Yao, S. Xu., 2022. Polystyrene nanoplastics induced cardiomyocyte apoptosis and myocardial inflammation in carp by promoting ROS production. Fish Shellfish Immun 125:1-8.

Wu P., Lin S., Cao G., Wu J., Jin H., Wang C., Wong M. H., Yang Z., Cai Z., 2022. Absorption, distribution, metabolism, excretion and toxicity of microplastics in the human body and health implications. J Hazard Mater 437: 129361.

Wu R. T., Cai Y. F., Chen Y. X., Yang Y. W., Xing S. C., Liao X. D., 2021. Occurrence of microplastic in livestock and poultry manure in South China. Environ Pollut 277: 116790.

Wu Y., Wang Y., Wu W., Yin D., Sun X., Guo X., Chen J., Mahmood T., Yan L., Yuan J., 2020. Effects of nicotinamide and sodium butyrate on meat quality and muscle ubiquitination degradation genes in broilers reared at a high stocking density. Poult Sci 99 (3): 1462-1470.

Xu S., Ma J., Ji R., Pan K., Miao A. J., 2020. Microplastics in aquatic environments: Occurrence, accumulation, and biological effects. Sci Total Environ 703: 134699.

Yang D., Zhu J., Zhou X., Pan D., Nan S., Yin R., Lei Q., Ma N., Zhu H., Chen J., Han L., Ding M., Ding Y., 2022. Polystyrene micro- and nano-particle coexposure injures fetal thalamus by inducing ROS-mediated cell apoptosis. Environ Int 166: 107362.

Yu G., Wang L. G., Han Y., He Q. Y., 2012. clusterProfiler: an R package for comparing biological themes among gene clusters. OMICS 16 (5): 284-287.

Yuan Z., Nag R., Cummins E., 2022. Human health concerns regarding microplastics in the aquatic environment - from marine to food systems. Science of The Total Environment, 823, 153730-.

Yuan Z., Nag R., Cummins E., 2022. Human health concerns regarding microplastics in the aquatic environment - from marine to food systems. Science of The Total Environment, 823, 153730-.

Zha Fugeng, Shang Mengxin, Ouyang Zhuozhi, Guo Xuetao, 2022. The aging behaviors and release of microplastics: A review. Gondwana Res 108: 60-71.

Zhang G. Q., Ma Q. G., Ji C., 2008. Effects of dietary inosinic acid on carcass characteristics, meat quality, and deposition of inosinic acid in broilers. Poult Sci 87 (7): 1364-1369.

Zhang T., Chen C., Xie K., Wang J., Pan Z., 2021. Current State of Metabolomics Research in Meat Quality Analysis and Authentication. Foods 10 (10).

Zhang T., Zhang S., Chen L., Ding H., Wu P., Zhang G., Xie K., Dai G., Wang J., 2020. UHPLC-MS/MS-Based Nontargeted Metabolomics Analysis Reveals Biomarkers Related to the Freshness of Chilled Chicken. Foods 9 (9).

Figure Legends

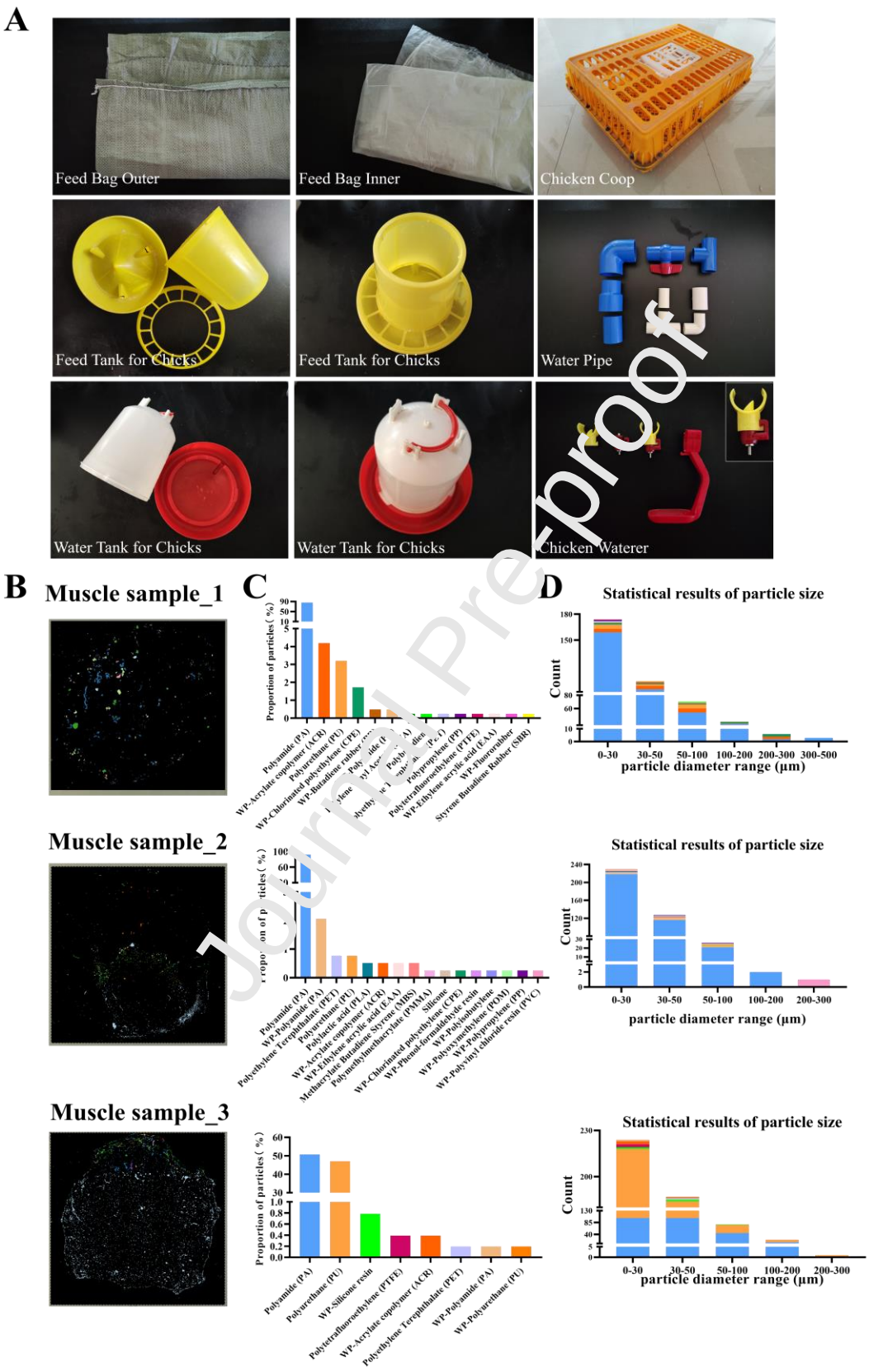

Figure 1. Microplastic residue can be detected in chicken skeletal muscle. (A) Potential

sources of microplastic pollution in chicken farms. (B) Microplastic identification images of chicken muscle by laser infrared imaging spectrometer (LDIR). (C) The proportion of different types of microplastics in chicken muscle samples. (D) Size distribution of microplastics detected in chicken muscle samples.

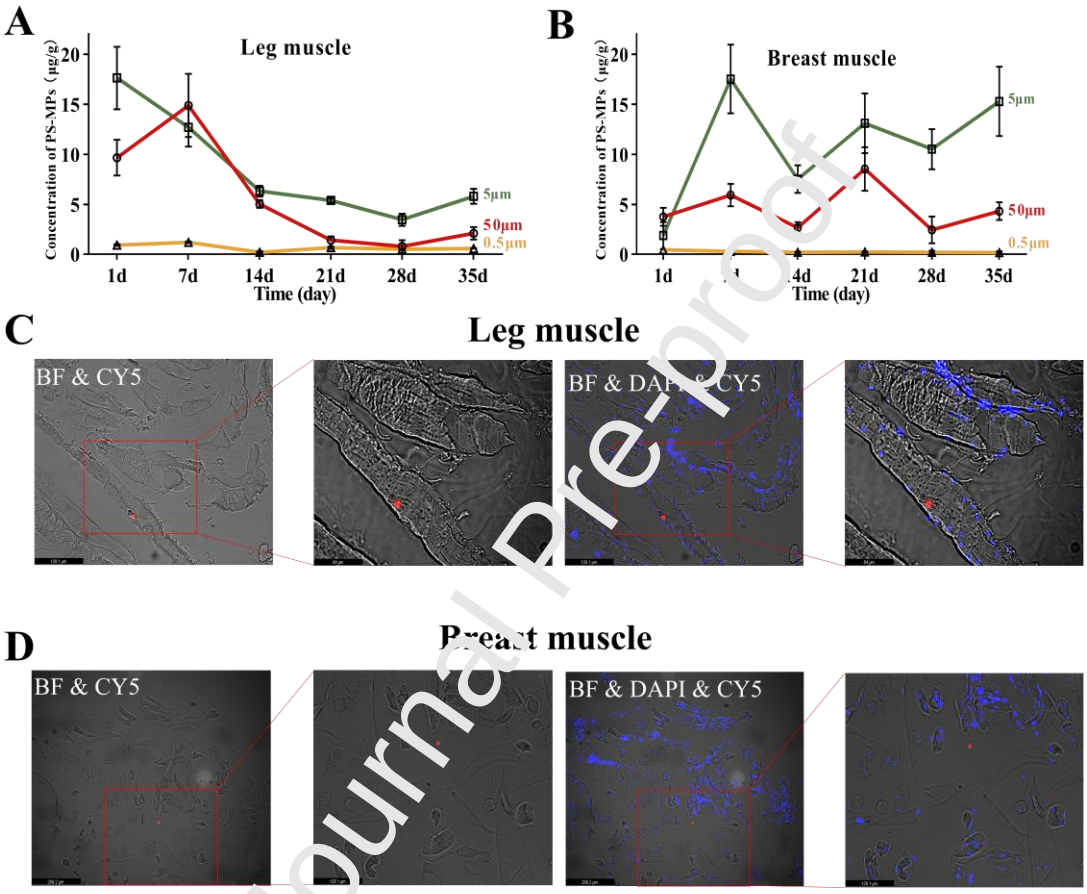

Figure 2. Characterization of microplastic ingestion and accumulation in chicken skeletal muscle. (A) The concentration of FPS-MPs in chicken leg muscle at different exposure times. (B) The concentration of FPS-MPs in chicken breast muscle at different exposure times. (C) Representative image of leg muscle section from chicken exposed for 5 μm FPS-MPs for 35 days. (D) Representative image of breast muscle section from chicken exposed for 5 μm FPS-MPs for 35 days. Red fluorescence (CY5) indicates FPS-MPs. Blue fluorescence (DAPI) represents the cell nucleus. BF means bright field. The results are shown

as the mean ± SEM. n = 4.

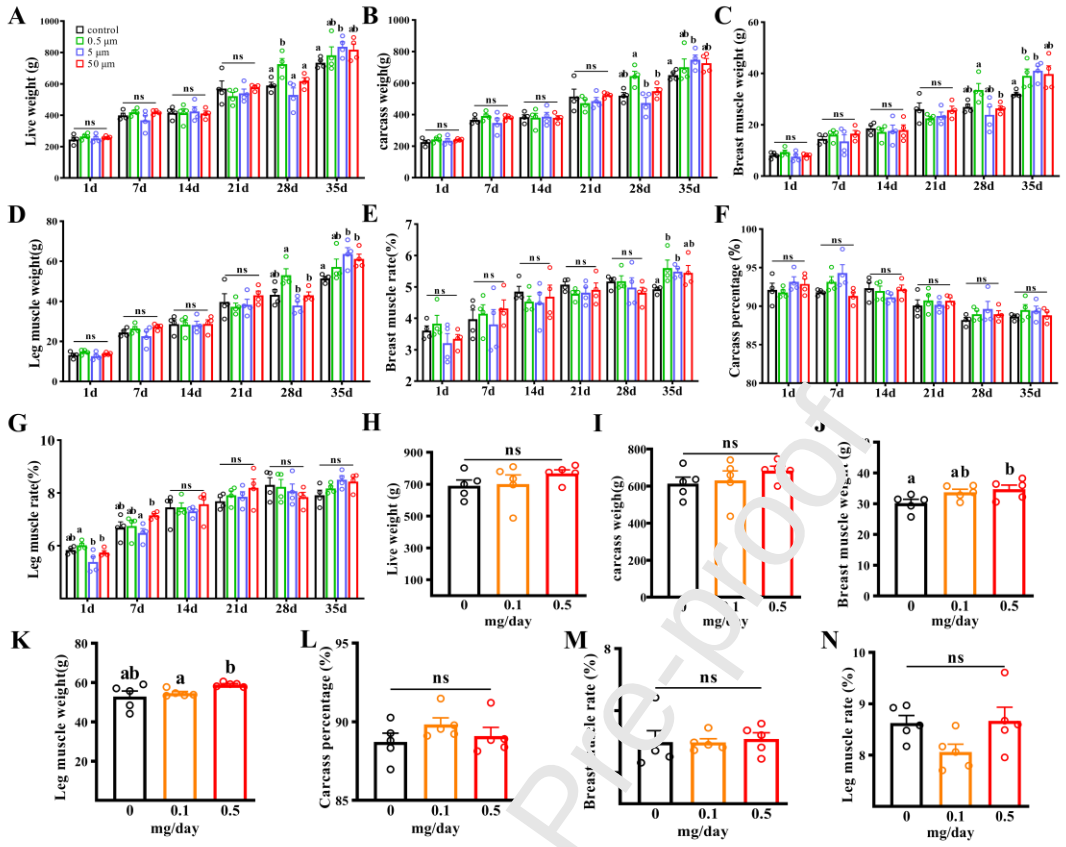

Figure 3. Microplastic accumulation promotes chicken muscle growth. (A-G) Effects of different sizes of FPS-MPs (0.1 mg/d) exposure on the live weight, carcass weight, breast muscle weight, leg muscle weight, breast muscle rate, carcass percentage, and leg muscle rate of chickens. (H-N) Effects of different concentrations of 5 μm PS-MPs exposure for 28 days on the live weight, carcass weight, breast muscle weight, leg muscle weight, carcass percentage, breast muscle rate, and leg muscle rate of chickens. The results are shown as the mean ± SEM. Different letters (a and b) indicate significant differences ($p < 0.05$) by Duncan's multiple range test. One-way ANOVA followed by Dunnett's test was used to compare differences in mean values at the 5% significance level.

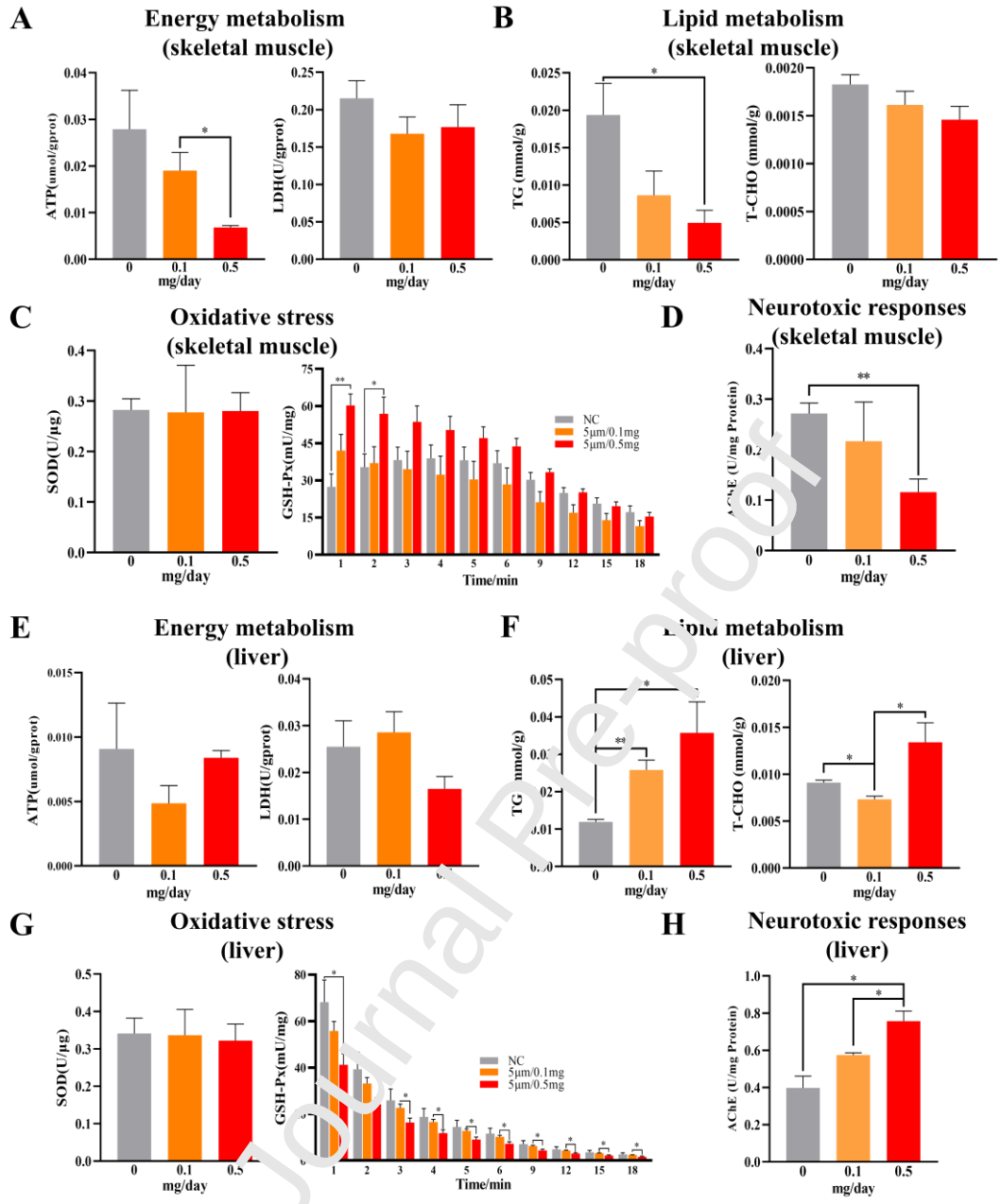

Figure 4. Effects of microplastic accumulation on chicken skeletal muscle and liver physiological function. (A) ATP levels and LDH activities of skeletal muscle. (B) TG and T-CHO levels of skeletal muscle. (C) SOD activities and GSH-Px levels of skeletal muscle. (D) SOD activities and GSH-Px levels of skeletal muscle. (E) ATP levels and LDH activities of the liver. (F) TG and T-CHO levels of liver. (G) SOD activities and GSH-Px levels of the liver. (H) SOD activities and GSH-Px levels of the liver. Chickens were fed different

concentrations of PS-MP for 28 days. The results are shown as the mean ± SEM. Independent sample *t*-tests were performed to determine the significance of differences between groups. **p* < 0.05; ***p* < 0.01. n=3.

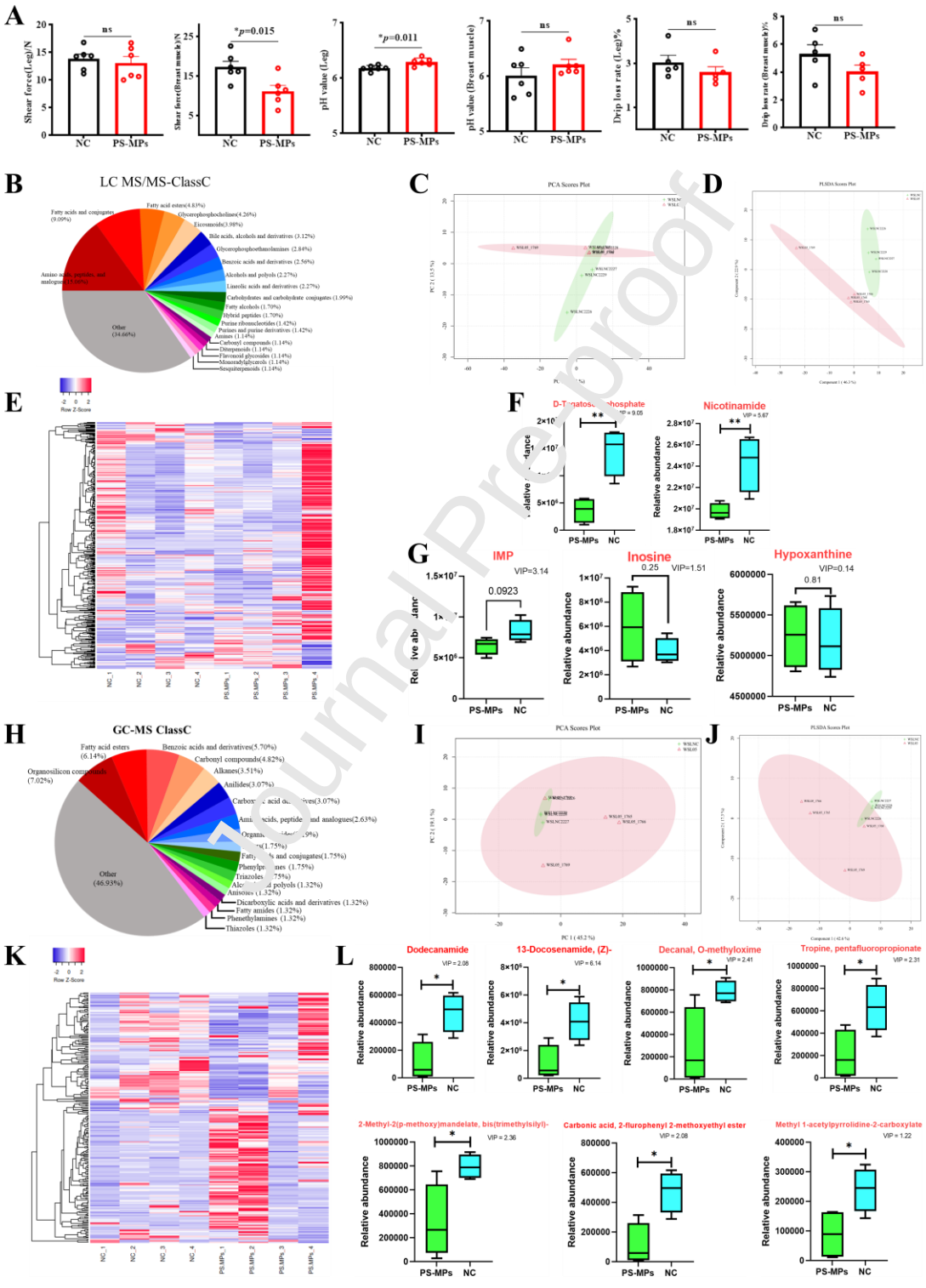

Figure 5. Microplastic feeding reduces chicken meat quality. (A) The meat quality

characteristics after PS-MPs feeding for 35 d. (B) The proportion of each metabolite detected by LC-MS/MS in chicken skeletal muscle. (C) PCA analysis of the two groups. WSL05 means chicken exposed to PS-MPs. WSLNC means control group. (D) PLS-DA analysis of the two groups. (E) Heatmap of metabolites detected by LC-MS/MS. (F) Metabolites significantly changed after PS-MP exposure. (G) Key metabolites associated with meat quality. (H) The proportion of each flavor substance detected by GC-MS in chicken skeletal muscle. (I) PCA analysis of the two groups. WSL05 means chicken exposed to PS-MPs. WSLNC means control group. (J) PLS-DA analysis of the two groups. (K) Heatmap of flavor substance detected by GC-MS. (L) The flavor substance significantly changed after PS-MPs exposure. The results are shown as the mean ± SEM. Independent sample t-tests were performed to determine the significance of differences between groups. $*p < 0.05$; $**p < 0.01$.

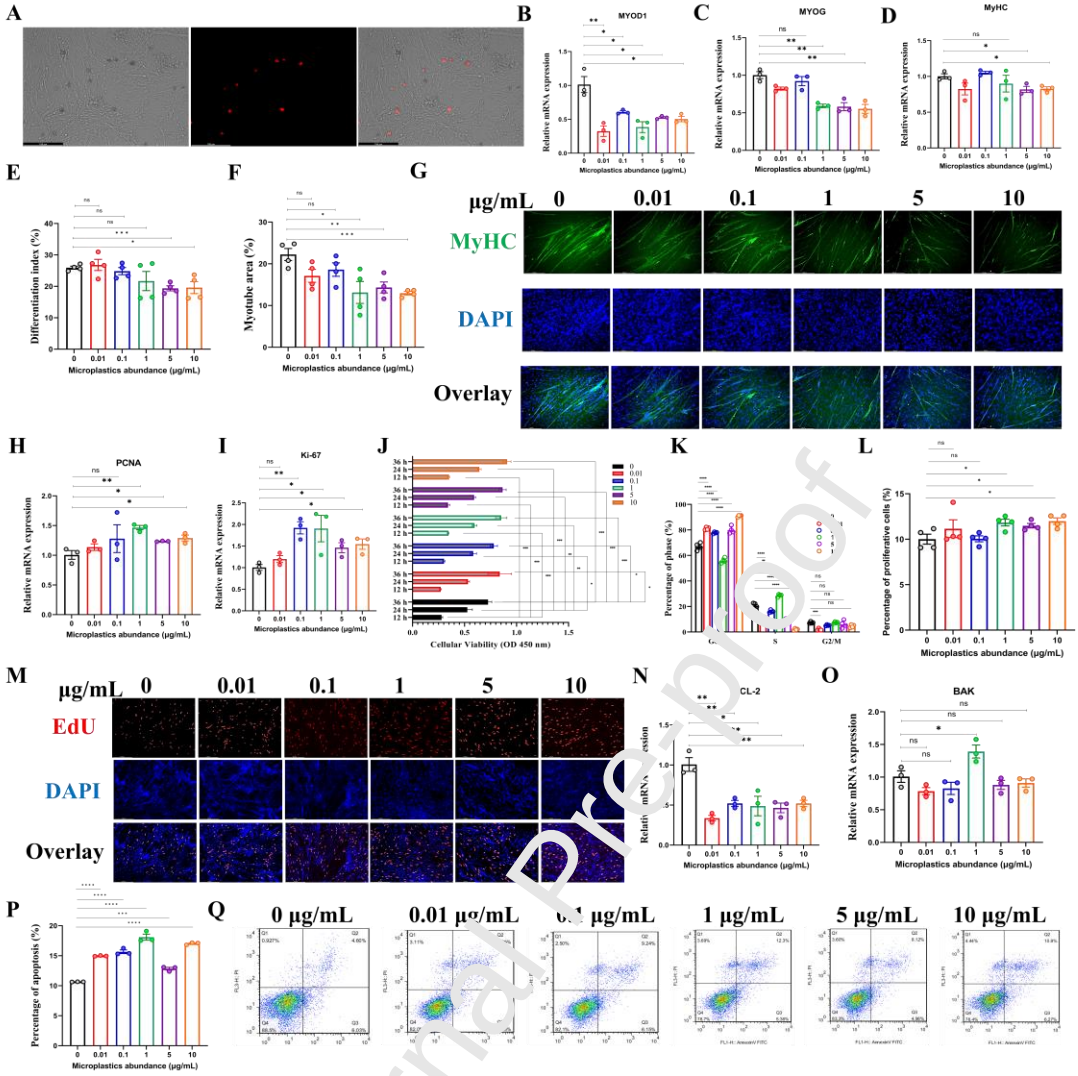

Figure 6. Microplastics induced myoblasts proliferation and apoptosis but decreased myoblasts differentiation. (A) Distribution of FPS-MPs in chicken primary myoblast. Red fluorescent represents FPS-MP. (B-D) Relative mRNA expression of muscle differentiation marker genes *MYOD1*, *MYOG*, and *MyHC* in chicken primary myoblasts exposed different abundances of FPS-MP. (E-F) Differentiation index and myotube area in chicken primary myoblasts exposed different abundances of FPS-MP. (G) MyHC staining of cells at 72 h after FPS-MP exposure in chicken primary myoblasts. Fused myotubes were positive for MyHC (green), and cell nuclei were positive for DAPI (blue). (H-I) Relative mRNA expression of cell proliferation marker genes *PCNA* and *Ki-67* in chicken primary myoblasts exposed

different abundances of FPS-MP. (J) Cell viability of chicken primary myoblasts exposed to a different abundance of FPS-MP. (K) Cell cycle analysis of chicken primary myoblasts after exposed different abundance of FPS-MP. (M) EdU staining of chicken primary myoblasts after exposed different abundances of FPS-MP. (N-O) Relative mRNA expression of cell apoptosis marker genes *BCL-2* and *BAK* in chicken primary myoblasts exposed different abundances of FPS-MP. (P-Q) Cell apoptosis analysis of chicken primary myoblasts after exposed different abundance of FPS-MPs. The results are shown as the mean ± SEM. Independent sample t-tests were performed to determine the significance of differences between groups. $*p < 0.05$; $**p < 0.01$.

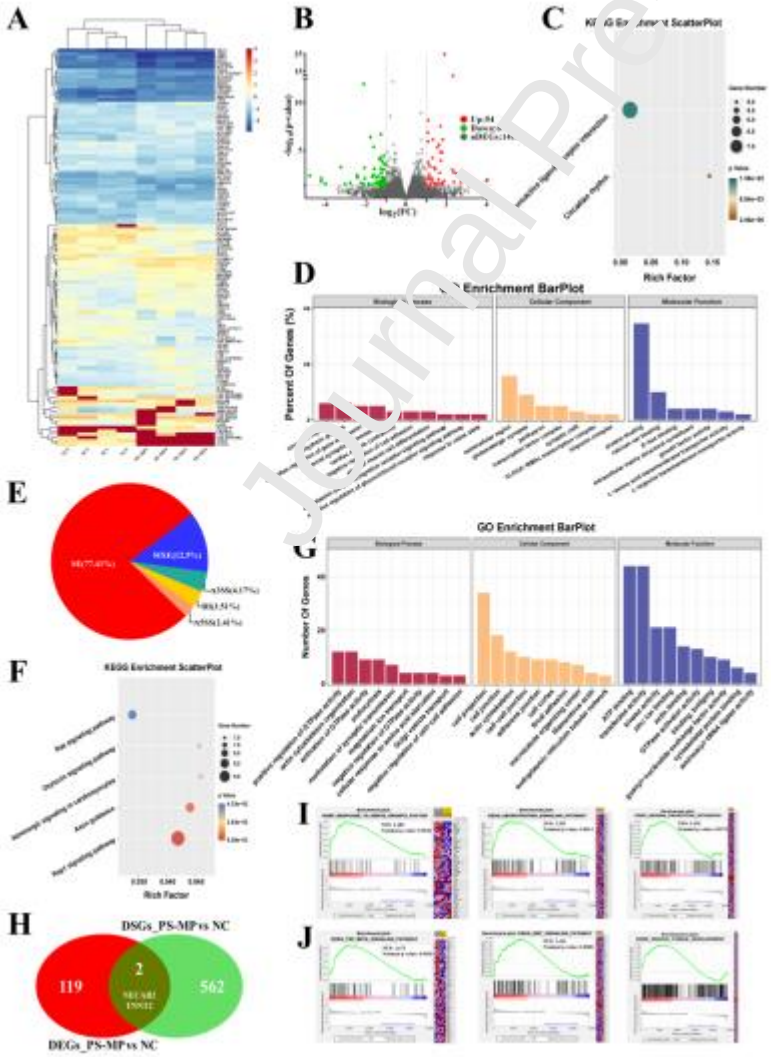

Figure 7. Transcriptome analysis reveals that PS-MP exposure affects chicken skeletal muscle function by regulating genes involved in neural function and muscle cell development. (A) Heat map of transcriptome expression of each sample. (B) The volcano plot shows DEGs between the two groups. (C) The significantly enriched KEGG pathways of DEGs. (D) Gene ontology enrichment of DEGs. (E) The proportion of various alternative splicing types of DSGs. SE: Skipped Exon. MXE: Mutually Exclusive Exons. A3SS: Alternative 3' Splice Site. RI: Retained Intron. A5SS: Alternative 5' Splice Site. (F) The significantly enriched KEGG pathways of DSGs. (G) Gene ontology enrichment of DSGs. (H) Venn diagram of DEGs and DSGs. (I-J) GSEA analysis of RNA-seq data from PS-MPs exposure chicken breast muscle and control chicken breast muscle.

Tissues	Numbers	MPs types & Abundance (mg/kg)								
		PS	**PET**	**PA6**	**PA66**	**PE**	**PMMA**	**PP**	**PVC**	**PC**
Jejunum	1	2.221	N.D.	488.07	476.548	N.D.	N.D.	N.D.	N.D.	N.D.
	2	2.349	N.D.	936.447	364.131	N.D.	N.D.	N.D.	N.D.	N.D.
	3	2.073	N.D.	300.903	N.D.	N.D.	N.D.	N.D.	N.D.	N.D.
	mean	**2.214**	**N.D.**	**575.140**	**420.340**	**N.D.**	**N.D.**	**N.D.**	**N.D.**	**N.D.**
Liver	1	7.416	2360.799	1321.291	169.51	N.D.	N.D.	N.D.	N.D.	N.D.
	2	3.816	1723.805	559.575	N.D.	N.D.	N.D.	N.D.	N.D.	N.D.
	3	6.186	1169.519	947.55	N.D.	N.D.	N.D.	N.D.	N.D.	N.D.
	mean	**5.806**	**1751.374**	**942.805**	**169.510**	**N.D.**	**N.D.**	**N.D.**	**N.D.**	**N.D.**
Leg muscle	1	3.997	N.D.	1308.325	N.D.	N.D.	N.D.	N.D.	N.D.	N.D.
	2	2.625	N.D.	645.195	N.D.	N.D.	N.D.	N.D.	N.D.	N.D.
	3	2.187	N.D.	700.617	N.D.	N.D.	N.D.	N.D.	N.D.	N.D.
	mean	**2.936**	**N.D.**	**884.712**	**N.D.**	**N.D.**	**N.D.**	**N.D.**	**N.D.**	**N.D.**
Breast muscle	1	1.712	N.D.	641.723	N.D.	N.D.	N.D.	N.D.	N.D.	N.D.
	2	7.491	N.D.	580.259	N.D.	N.D.	N.D.	N.D.	N.D.	N.D.
	3	2.883	N.D.	462.79	N.D.	N.D.	N.D.	N.D.	N.D.	N.D.

Table 1. Statistical analysis of MP types and abundance in chicken tissues

mean	**4.029**	**N.D.**	**561.593**	**N.D.**	**N.D.**	**N.D.**	**N.D.**	**N.D.**	**N.D.**

N.D.: not detectable

Graphical abstract

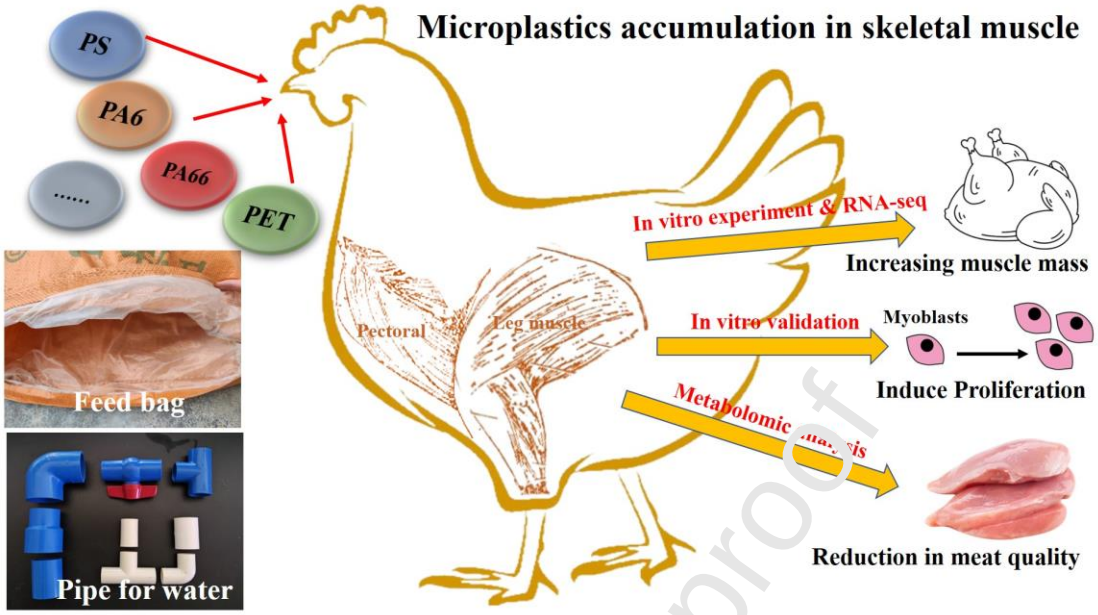

Highlights

- Microplastics accumulate in the muscles of farmed broilers.
- Polystyrene microplastics (PS-MPs) promote the muscle growth of broilers.
- PS-MP exposure reduced meat quality but increased the muscle weight of chickens.
- PS-MPs feeding can affect the expression of genes related to neural function.